

Resonance Raman scattering of Si local vibrational modes in GaAs

M. Ramsteiner, J. Wagner, H. Ennen, and M. Maier

Fraunhofer-Institut für Angewandte Festkörperphysik, Eckerstrasse 4, D-7800 Freiburg, West Germany

(Received 17 March 1988)

We have studied the resonance of Raman scattering by Si local vibrational modes (LVM's) in heavily doped GaAs prepared by ion implantation and rapid thermal annealing. For photon energies (1.9–2.7 eV) approaching the E_1 energy gap, similar resonance behavior was found for scattering by the Si on As site (Si_{As}) LVM and by the longitudinal-optical phonon. Compared with undoped GaAs, both resonances are reduced in peak height and are broadened. This can be understood on the basis of a lowering and broadening of the $(E_1, E_1 + \Delta_1)$ gap resonance due to residual implantation damage and due to the high dopant concentration. Scattering by the Si on Ga site (Si_{Ga}) LVM, in contrast, shows no resonance enhancement for the above range of photon energies. However, excitation at 3.00 eV, which is almost in resonance with the E_1 gap energy, also enhances scattering by the Si_{Ga} LVM, indicating a rather narrow E_1 gap resonance for that LVM. Taking advantage of that resonance we observe also Raman scattering by the Si_{Ga} LVM in heavily doped GaAs layers grown by molecular-beam epitaxy down to a Si concentration of $\sim 10^{18} \text{ cm}^{-3}$.

I. INTRODUCTION

Defect-induced local vibrational modes (LVM's) in GaAs have been studied extensively by infrared absorption.^{1,2} Recently also Raman scattering has been used to investigate the LVM of Si,^{3–5} P,⁶ and a pseudolocalized intrinsic defect mode⁷ in GaAs. Among these impurities Si is of particular interest as it can occupy both the Ga (Si_{Ga}) and the As (Si_{As}) lattice site.^{8,9} Besides the Si_{Ga} and the Si_{As} LVM another Si-related defect mode is Raman active caused by the vibration of next neighboring Si_{Ga} - Si_{As} pairs.^{3–5} The most detailed Raman studies of Si LVM's in GaAs have been carried out using samples prepared by ion implantation with doses in the range 5×10^{14} to $1 \times 10^{16} \text{ cm}^{-2}$ followed by thermal annealing.^{3,4} There is only one report of Raman scattering by Si LVM's in epitaxial layers grown by liquid-phase epitaxy⁵ and no LVM Raman data have been reported so far on high-quality Si-doped molecular-beam-epitaxial (MBE) layers. These GaAs:Si layers, however, show good electrical activation and Si LVM's have been successfully studied in such samples by infrared absorption.¹⁰

The purpose of the present work was to investigate the resonance of the Raman scattering by Si LVM's in ion-implanted and annealed GaAs and to extend the Raman spectroscopy of Si LVM's to epitaxial layers grown by MBE. The organization of the paper is as follows: Section II describes the experimental details. Section III A contains the experimental results and the discussion for Si-ion-implanted GaAs and Sec. III B covers the work on Si-doped MBE layers. The conclusions are given in Sec. IV.

II. EXPERIMENTAL

The ion-implanted samples were prepared by implantation of ^{29}Si into undoped semi-insulating GaAs substrates

grown by the liquid-encapsulated Czochralski technique. The ion energy was 120 keV and the doses ranged from 5×10^{14} to $1 \times 10^{16} \text{ cm}^{-2}$. The beam current density varied between 40 and 100 nA/cm², depending on the total ion dose. Annealing was performed in a rapid thermal annealing furnace with the sample surface protected by the proximity technique—i.e., the sample placed face down on another GaAs wafer. The peak temperature of 800–850 °C was maintained for 2–5 sec. The results discussed below are independent of the details of the annealing.

The heavily Si-doped MBE layers were grown at a substrate temperature of 560 °C. The thickness of the layers is $\sim 1 \mu\text{m}$. The charge carrier concentrations were determined by Hall-effect measurements and from the frequency of the coupled longitudinal-optical (LO) -phonon-plasmon mode in the Raman spectrum.¹¹ They are listed in Table I together with the Si concentrations obtained from secondary-ion mass spectrometry (SIMS).

The Raman experiments were carried out in back-scattering geometry from a (100) surface. The spectra were excited with several lines of a Kr^+ laser and an Ar^+ laser covering the range of photon energies from 1.92 to 3.00 eV. In crystalline GaAs the probing depth $1/(2\alpha)$, where α denotes the absorption coefficient, amounts to $\sim 140 \text{ nm}$ for the lowest and $\sim 8 \text{ nm}$ for the highest photon energy used.¹² The scattered light was filtered and dispersed in a triple monochromator and detected with an intensified silicon diode array.

III. RESULTS AND DISCUSSION

A. Ion-implanted GaAs

The Raman spectrum of GaAs implanted with $^{29}\text{Si}^+$ at a dose of $1 \times 10^{16} \text{ cm}^{-2}$ followed by rapid thermal annealing is displayed in Fig. 1. The spectrum was recorded at room temperature with the incident light polarized along

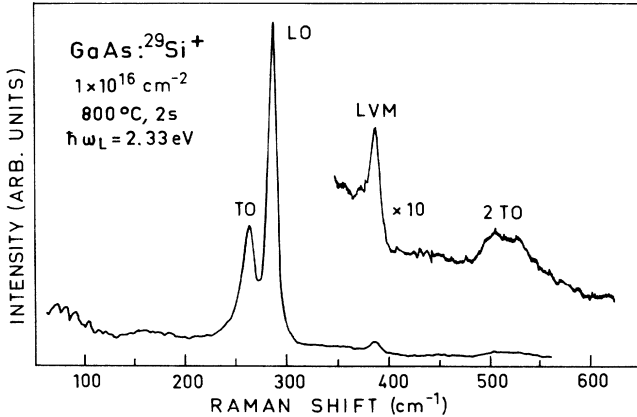


FIG. 1. Room-temperature Raman spectrum of Si^+ -implanted and rapidly thermal annealed GaAs. The implantation energy and dose were 120 keV and $1 \times 10^{16} \text{ cm}^{-2}$, respectively. The annealing temperature of 800 °C was maintained for 2 sec. The spectrum was excited at 2.33 eV and recorded with a spectral resolution of 5 cm^{-1} . LO, TO, and 2TO denote Raman scattering by intrinsic phonons. LVM indicates Raman scattering by the $^{29}\text{Si}_{\text{As}}$. LVM.

a $\langle 100 \rangle$ direction and the scattered light not analyzed for its polarization. Besides intrinsic first-order scattering by longitudinal-optical and by transverse-optical (TO) phonons, and second-order scattering by two TO phonons¹³ the spectrum shows an extrinsic Raman line at 390 cm^{-1} labeled LVM. This line arises from Raman scattering by the LVM of ^{29}Si on the As site ($^{29}\text{Si}_{\text{As}}$). This assignment is based on the LVM frequency of 396 cm^{-1} for $^{28}\text{Si}_{\text{As}}$ at 300 K (Ref. 4) and on a frequency down shift of 5.5 cm^{-1} due to the ^{29}Si - ^{28}Si isotope mass effect (Ref. 8).

The relatively large intensity of the TO-phonon line, which is forbidden for backscattering from a (100) face of a perfect crystal, indicates a considerable amount of residual implantation damage in the material. We have to note that we observe such a spectrum with sharp crystalline Raman lines only after sample annealing. In the as-implanted material exposed to doses exceeding 10^{15} cm^{-2} we observe the spectrum of amorphous GaAs indicating a heavily damaged surface layer.¹⁴ This is in contrast to the data reported by Holtz *et al.*,⁴ who found for an implantation dose of 10^{16} cm^{-2} crystalline features in the Raman spectrum even in the as-implanted material. A possible explanation for this discrepancy might be some unintentional heating of the substrate during the implantation. Even modest heating during implantation may lead to crystalline features in the Raman spectrum, which would show only amorphous structures otherwise.¹⁵

Figure 2 displays the LVM Raman spectrum for different implantation doses ranging from $1 \times 10^{16} \text{ cm}^{-2}$ [curve shown in (a)] to $5 \times 10^{14} \text{ cm}^{-2}$ [curve shown in (d)]. The spectra, recorded with excitation at 2.33 eV, show the $^{29}\text{Si}_{\text{As}}$ peak as the dominant LVM Raman line for all doses $< 10^{16} \text{ cm}^{-2}$ with the other possible LVM lines ($^{29}\text{Si}_{\text{Ga}}$ and $^{29}\text{Si}_{\text{As}}\text{-}^{29}\text{Si}_{\text{Ga}}$) below the noise limit. For the sample with the highest dose ($1 \times 10^{16} \text{ cm}^{-2}$) a low-frequency shoulder of the $^{29}\text{Si}_{\text{As}}$ peak can be assigned to

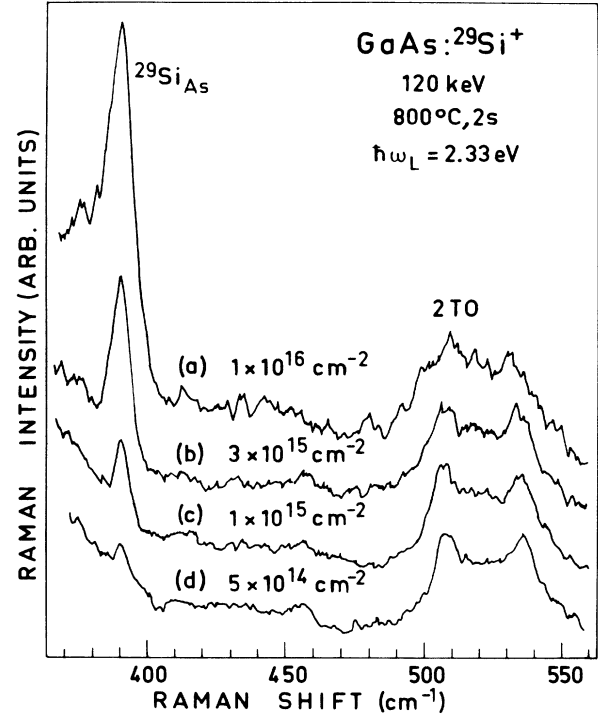


FIG. 2. Room-temperature Raman spectra of Si^+ -implanted and rapidly thermal annealed GaAs. The implantation energy was 120 keV. The different doses are given in the figure. The annealing temperature of 800 °C was maintained for 2 sec. The spectra were excited at 2.33 eV and recorded in the $x(y,z)\bar{x}$ scattering configuration with a spectral resolution of 3.5 cm^{-1} . 2TO indicates intrinsic second-order transverse-optical-phonon scattering and $^{29}\text{Si}_{\text{As}}$ denotes Raman scattering by the $^{29}\text{Si}_{\text{As}}$ LVM.

some contribution of scattering by the $^{29}\text{Si}_{\text{As}}\text{-}^{29}\text{Si}_{\text{Ga}}$ pair LVM and/or by the $^{29}\text{Si}_{\text{Ga}}$ LVM. The integrated intensity of the $^{29}\text{Si}_{\text{As}}$ LVM Raman line normalized to the integrated intensity of the dipole-allowed LO-phonon line is plotted in Fig. 3 versus the implantation dose. A linear correlation is found. This is in contrast to the result reported by Holtz *et al.*,⁴ who found a sublinear increase

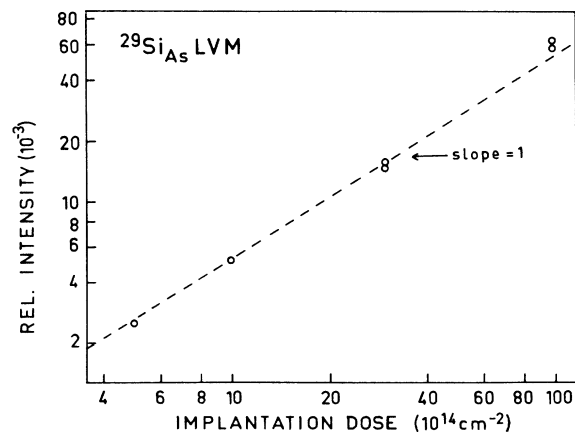


FIG. 3. Intensity of the $^{29}\text{Si}_{\text{As}}$ LVM relative to the strength of the dipole-allowed LO-phonon scattering vs implantation dose.

of the Si LVM intensity with implantation dose described by a power law with an exponent of 0.7. A linear dependence, as found in the present study, is expected if the following conditions are fulfilled: (i) the concentration of Si_{As} is proportional to the total Si concentration, (ii) the Raman scattering cross section per Si_{As} is independent of the Si concentration, and (iii) the dopant profile is identical for all implantation doses. The last condition is fulfilled as checked by SIMS (see below). Concerning the first two points we can only state that the scattering cross section multiplied by the ratio of the Si_{As} to the total Si concentration must be constant to explain a linear correlation. Assuming a Si_{As} concentration proportional to the total Si content this would imply a concentration-independent scattering cross section for the Si_{As} LVM.

For Raman scattering by the boron LVM in crystalline silicon Chandrasekar *et al.*¹⁶ found a decrease of the LVM scattering cross section with the boron concentration N_{B} proportional to $N_{\text{B}}^{-2/3}$. They attributed this decrease to screening effects due to the increasing concentration of free holes which is equal to the boron concentration. This screening reduces the polarizability of the Si—B bonds. In the present case of heavily Si-doped GaAs prepared by ion implantation the concentration of free carriers is much lower than the Si concentration due to the poor electrical activation of the dopant.³ Therefore such screening effects are expected to be less prom-

inent in the present case making a constant scattering cross section plausible.

Figure 4 shows the $^{29}\text{Si}_{\text{As}}$ LVM line recorded at 15 K with a spectral resolution of 2.3 cm^{-1} for two different samples implanted with doses of $1 \times 10^{16} \text{ cm}^{-2}$ [Fig. 4(a)] and $3 \times 10^{15} \text{ cm}^{-2}$ [Fig. 4(b)]. The scattering configuration used was $x(y,z)\bar{x}$. Here x , y , and z denote $\langle 100 \rangle$ crystallographic directions. For this configuration only scattering described by a Raman tensor with $\Gamma_{15} + \Gamma_{25}$ symmetry is allowed.¹⁷ This suppresses the Γ_1 component of the intrinsic second-order phonon spectrum¹³ with respect to the $^{29}\text{Si}_{\text{As}}$ LVM line (Γ_{15} symmetry).³ The measured width of the LVM line increases from 5 to 10 cm^{-1} when increasing the implantation dose from 3×10^{15} to $1 \times 10^{16} \text{ cm}^{-2}$. The larger LVM linewidth for the highest dose indicates an additional broadening due to residual implantation damage and due to the high dopant concentration.

The dependence of the Si LVM Raman spectrum on the incident photon energy is displayed in Fig. 5. For excitation at 1.92 eV two LVM peaks at 378 and 390 cm^{-1} are observed with about equal intensity which arise from scattering by the $^{29}\text{Si}_{\text{Ga}}$ and the $^{29}\text{Si}_{\text{As}}$ LVM's, respectively. Increasing the incident photon energy to 2.18 eV the $^{29}\text{Si}_{\text{As}}$ LVM line becomes dominant and the $^{29}\text{Si}_{\text{Ga}}$ line is

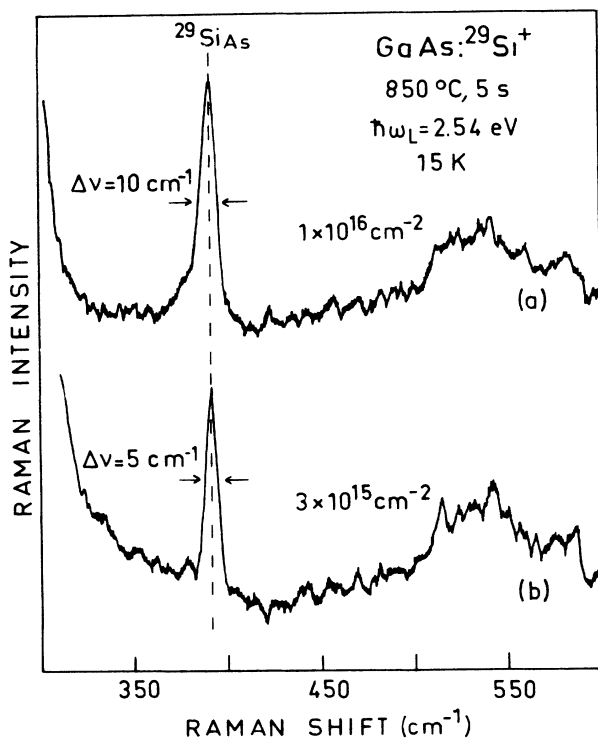


FIG. 4. Low-temperature (15 K) Raman spectra of Si^+ -implanted and rapidly thermal annealed GaAs. The implantation energy was 120 keV. The doses were (a) $1 \times 10^{16} \text{ cm}^{-2}$ and (b) $3 \times 10^{15} \text{ cm}^{-2}$, respectively. The annealing temperature of 850°C was maintained for 5 sec. The spectra were excited at 2.54 eV and recorded with a spectral resolution of 2.3 cm^{-1} . The scattering configuration was $x(y,z)\bar{x}$. $^{29}\text{Si}_{\text{As}}$ denotes the $^{29}\text{Si}_{\text{As}}$ LVM Raman line.

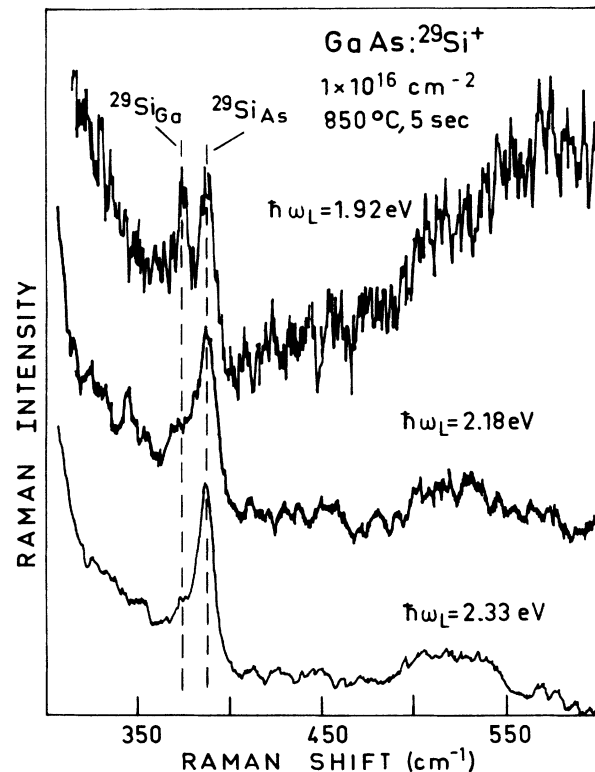


FIG. 5. Room-temperature Raman spectra of Si^+ -implanted and annealed GaAs excited with different photon energies indicated in the figure. The implantation energy and dose were 120 keV and $1 \times 10^{16} \text{ cm}^{-2}$, respectively. The annealing temperature of 850°C was maintained for 5 sec. The spectral resolution varied between 3.5 and 5 cm^{-1} for the lowest and highest photon energy, respectively. $^{29}\text{Si}_{\text{Ga}}$ and $^{29}\text{Si}_{\text{As}}$ indicate Raman scattering by the $^{29}\text{Si}_{\text{Ga}}$ and $^{29}\text{Si}_{\text{As}}$ LVM's.

only seen as a low-frequency shoulder of the $^{29}\text{Si}_{\text{As}}$ peak. For excitation at 2.33 eV the intensity of the $^{29}\text{Si}_{\text{Ga}}$ LVM decreases further and for an incident photon energy of 2.54 eV only the $^{29}\text{Si}_{\text{As}}$ LVM line is observed (see Fig. 4). Here we have to note that with varying photon energy also the probing depth $1/(2\alpha)$ changes (see Sec. II). Therefore the change in the LVM Raman spectrum may arise from different depth profiles of $^{29}\text{Si}_{\text{As}}$ and $^{29}\text{Si}_{\text{Ga}}$ in the implanted layer with an enrichment of $^{29}\text{Si}_{\text{As}}$ close to the surface. Alternatively the cross section for Raman scattering by the $^{29}\text{Si}_{\text{As}}$ LVM may have a much stronger ($E_1, E_1 + \Delta_1$) gap resonance than the cross section for scattering by the $^{29}\text{Si}_{\text{Ga}}$ LVM.

To clarify that point we performed the following experiments. First we removed the implanted layer on a sample in steps of 23 nm each by sputtering with Ar ions and measured after each step the Si LVM Raman spectrum with excitation at 2.71 eV. For this photon energy the probing depth $1/(2\alpha)$ of ~ 40 nm is comparable to the step size of the sputter removal. In all the spectra we observe only scattering by the $^{29}\text{Si}_{\text{As}}$ LVM and the variation of the LVM scattering intensity with sputter depth clearly reproduces the depth profile of the total Si concentration measured by SIMS (see below). Second we measured the Si LVM Raman spectrum on a cleaved cross section of the implanted layer. Here the diameter of the focus of the exciting laser ($\sim 70 \mu\text{m}$) is much larger than the thickness of the implanted layer of $\sim 0.25 \mu\text{m}$ (see Fig. 7). Therefore, in this experiment we average over the whole depth of the implanted layer. Because of the very low Si LVM scattering intensity caused by the considerable mismatch between the excited area ($\sim 70 \mu\text{m}$ in diameter) and the width ($\sim 0.25 \mu\text{m}$) of the implanted layer, Si LVM spectra could only be recorded with a sufficient signal-to-noise ratio for exciting photon energies ≥ 2.5 eV. Again the Raman spectra show only scattering by the $^{29}\text{Si}_{\text{As}}$ LVM. Based on these two experiments we conclude (a) that the $^{29}\text{Si}_{\text{As}}$ depth profile follows the depth distribution of Si measured by SIMS and (b) that the ($E_1, E_1 + \Delta_1$) gap resonance of the LVM scattering cross section is different for Si_{As} and Si_{Ga} . If we take into account that, averaged over the whole depth of the implanted layer, the concentration of $^{29}\text{Si}_{\text{Ga}}$ is about four times higher than that of $^{29}\text{Si}_{\text{As}}$ (Ref. 18) it is evident that the absolute values of both scattering cross sections must be quite different.

The situation gets even more complicated when we excite the Raman spectra at 3.00 eV, which is almost in resonance with the E_1 gap energy [2.89 eV at 300 K,¹⁹ 3.03 eV at 77 K (Ref. 20)]. Such spectra are displayed in Fig. 6. At 300 K only the $^{29}\text{Si}_{\text{Ga}}$ LVM is resolved just above the noise level. Cooling the sample down to 77 K the LVM spectrum is much better resolved and scattering by both the $^{29}\text{Si}_{\text{As}}$ and the $^{29}\text{Si}_{\text{Ga}}$ LVM is observed at about equal intensity. The scattering intensity of the $^{29}\text{Si}_{\text{As}}$ LVM measured relative to intrinsic phonon scattering is much lower for excitation at 3.00 eV compared to excitation at 1.9–2.7 eV. This is due to the fact that within the probing depth (~ 10 nm) of light with 3.00 eV photon energy the Si concentration is only a small fraction of the

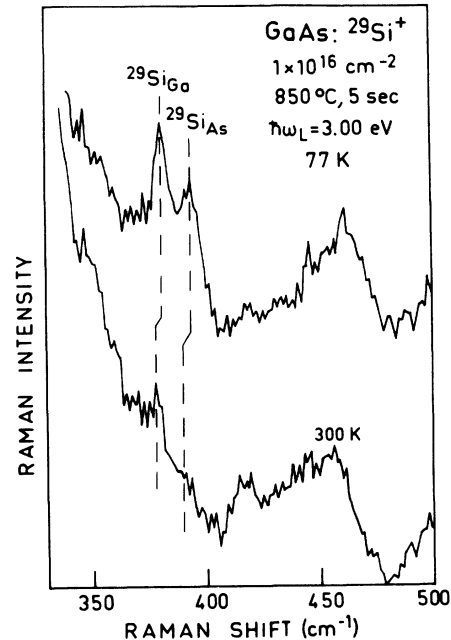


FIG. 6. Raman spectra of Si^+ -implanted and annealed GaAs excited at 3.00 eV. The sample was kept at 300 K (bottom) and 77 K (top), respectively. The spectra were recorded with a spectral resolution of 5 cm^{-1} in the $x(y,z)\bar{x}$ scattering configuration. The expected frequencies of the $^{29}\text{Si}_{\text{Ga}}$ and $^{29}\text{Si}_{\text{As}}$ LVM's at 77 and 300 K are indicated in the figure.

peak concentration (see Fig. 7). The enhancement of the Si LVM spectrum at 77 K relative to the spectrum recorded at 300 K may be due to the fact that at 77 K excitation at 3.00 eV is closer to the E_1 gap resonance than at 300 K.

In order to evaluate the dispersion of the cross section for Raman scattering by the $^{29}\text{Si}_{\text{As}}$ and $^{29}\text{Si}_{\text{Ga}}$ LVM one has to take into account the depth distribution of the implanted Si atoms. The depth profile of ^{29}Si as measured by SIMS is shown in Fig. 7(a). Due to the transient behavior of the secondary-ion yield at the beginning of sputter removal the measured profile has been extrapolated towards the surface by fitting a Gaussian to the maximum of the SIMS profile. For comparison also the depth dependence of the Raman sensitivity is plotted for different incident photon energies. These curves are given by the absorption of the incident and scattered light and can be written as $\exp(-2\alpha x)$ where x is the distance from the surface. Here we assumed a small Stokes shift of the scattered light such that for the incident and the scattered light α is approximately the same. Figure 7(b) shows the Si depth profile weighted with the Raman sensitivity and it is clearly seen that for different incident photon energies different portions of the Si depth profile are probed.

To correct for this effect the measured Si LVM intensity was multiplied by $f(\hbar\omega)$ with

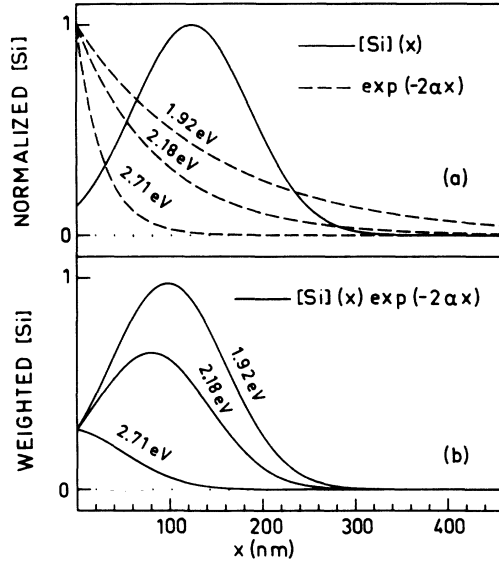


FIG. 7. (a) Concentration of the implanted Si ($[Si](x)$) vs depth x . $[Si](x)$ was measured by SIMS. For comparison also the Raman sensitivity $[\exp(-2\alpha x)]$ is plotted for different incident photon energies indicated in the figure. Here α denotes the absorption coefficient. (b) The bottom part shows the Si concentration multiplied by the Raman sensitivity for different incident photon energies.

$$f(\hbar\omega) = \frac{\int_0^\infty [Si](x) \exp[-2\alpha(\hbar\omega)x] dx}{\int_0^\infty \exp[-2\alpha(\hbar\omega)x] dx} = 2\alpha(\hbar\omega) \int_0^\infty [Si](x) \exp[-2\alpha(\hbar\omega)x] dx. \quad (1)$$

Here $\hbar\omega$ denotes the incident photon energy and $[Si](x)$ is the Si depth profile normalized to a peak concentration of 1. This correction implies that the depth profile of the total Si content measured by SIMS and the profile of Si_{As} and Si_{Ga} are identical. As discussed above Raman depth profiling of the $^{29}Si_{As}$ LVM did show that this assumption is justified at least for Si_{As} .

For the measurement of the Raman scattering efficiencies crystalline silicon was used as a reference scatterer¹⁷ and the dispersion of the corresponding Raman tensor matrix element $|a|$ was taken from Ref. 21. To correct for the dispersion of the dielectric function ϵ ,²¹ ellipsometric data¹² were used for both GaAs and crystalline silicon. Here the assumption enters that the dispersion of ϵ for heavily Si-doped GaAs prepared by

$$|a| = \left| A_1 \left\{ -g(x_0) + \frac{4E_0}{\Delta_0} \left[f(x_0) - \left(\frac{E_0}{E_0 + \Delta_0} \right)^{3/2} f(x_{0s}) \right] \right\} + A_2 \left[\frac{1}{1-x_1^2} + \left(\frac{E_1}{E_1 + \Delta_1} \right)^2 \frac{1}{1-x_{1s}^2} \right] + A_3 \right| \quad (2)$$

with

$$g(x) = x^{-2} [2 - (1+x)^{-1/2} - (1-x)^{-1/2}],$$

$$f(x) = x^{-2} [2 - (1+x)^{1/2} - (1-x)^{1/2}],$$

and $x_j = \hbar\omega/E_j$, $A_1 = 7 \text{ \AA}^2$, $A_2 = 18 \text{ \AA}^2$, $A_3 = -5 \text{ \AA}^2$.

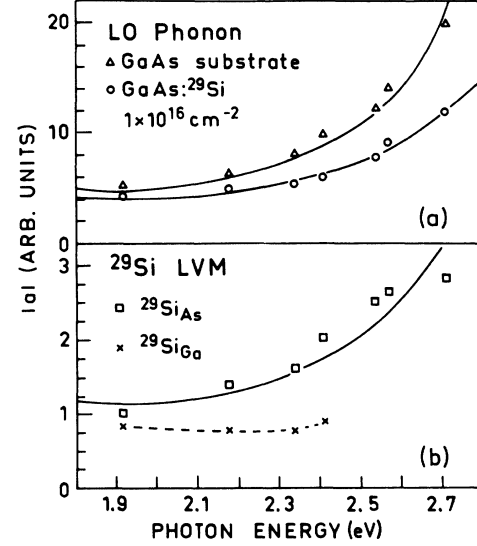


FIG. 8. (a) Raman tensor element $|a|$ for dipole-allowed Raman scattering by LO phonons in undoped (Δ) and Si-implanted and annealed GaAs (\circ). (b) Raman tensor element $|a|$ for Raman scattering by the $^{29}Si_{As}$ (\square) and the $^{29}Si_{Ga}$ (\times) LVM's. The data were recorded from undoped (LO phonon) and from $1 \times 10^{16} \text{ Si}^+/\text{cm}^2$ -implanted and rapidly thermal annealed (LO phonon and LVM) GaAs, respectively. The drawn curves were calculated using Eqs. (2) and (3). The broadening Γ was determined to 0.16 eV for the Si-implanted sample. The dashed curve is shown to guide the eye.

ion implantation can be approximated by the dispersion in undoped GaAs.

Figure 8(a) shows the dispersion of $|a|$ for dipole-allowed LO-phonon scattering in the undoped substrate and in the sample implanted with $1 \times 10^{16} \text{ Si}^+/\text{cm}^2$. It is clearly seen that the resonance enhancement of $|a|$ for photon energies approaching the E_1 gap energy of 2.89 eV is lower in the implanted and annealed sample than in the undoped material. Figure 8(b) shows the dispersion of $|a|$ for scattering by the $^{29}Si_{As}$ and the $^{29}Si_{Ga}$ LVM in the implanted sample. The data for excitation at 3.00 eV were omitted because, for the small probing depth of ~ 10 nm related to that photon energy, the SIMS data for the Si depth profile are not accurate enough to perform the correction described in Eq. (1).

The dispersion of $|a|$ for scattering by TO—as well as by LO phonons—in GaAs can be approximated sufficiently far from the resonance ($|\hbar\omega - E_j| > \Gamma_j$, where Γ_j is the lifetime broadening of the electronic transitions E_j) by^{19,22}

For the various gap energies E_j the following values were taken:¹⁹ $E_0 = 1.43$ eV, $\Delta_0 = 0.34$ eV, $E_1 = 2.89$ eV, $\Delta_1 = 0.23$ eV. The resulting theoretical curve is also shown in Fig. 8(a). Using a scaling factor as an adjustable parameter a good agreement is found with the exper-

imental data for LO-phonon scattering in the undoped sample but Eq. (2) fails to describe the dispersion of $|a|$ in the Si-implanted material. Therefore we introduced a finite Lorentzian broadening Γ of the various gaps to account for a doping-induced broadening of the corresponding Raman resonances.²³ Consequently we have to introduce in Eq. (2)

$$E'_j = E_j - i\Gamma \quad \text{and} \quad x'_j = \frac{\hbar\omega}{E_j - i\Gamma}. \quad (3)$$

For simplicity the same broadening Γ was used for all gaps. Using Γ and a scaling factor as adjustable parameters we fitted the experimental data for $|a|$ of the Si-implanted sample as shown in Fig. 8(a). With $\Gamma = 0.16$ eV and a reduction of the scaling factor by 30% with respect to undoped GaAs a good agreement is found between the theoretical curve and the experimental data. The present broadening of 0.16 eV is comparable to the one found for the $(E_1, E_1 + \Delta_1)$ gap resonance of first-order Raman scattering in P-implanted and laser-annealed Ge.²³

In Fig. 8(b) the same resonance curve ($\Gamma = 0.16$ eV) is plotted with a different scaling factor and it is seen that the dispersion of $|a|$ for scattering by the $^{29}\text{Si}_{\text{As}}$ LVM is reproduced, within the scatter of the experimental data points, by the theory. Therefore we can conclude that, within the experimental accuracy, the same E_1 gap resonance is found for scattering by LO phonon and by the $^{29}\text{Si}_{\text{As}}$ LVM for the above range of photon energies (1.9–2.7 eV). For scattering by the $^{29}\text{Si}_{\text{Ga}}$ LVM, in contrast, no resonance enhancement is found within the range of photon energies (1.9–2.4 eV) where this scattering is resolved.

Now we have to discuss how the Si LVM spectra excited at 3.00 eV (Fig. 6) fit into the above picture. Assuming that the LO-phonon-like $(E_1, E_1 + \Delta_1)$ gap resonance of the $^{29}\text{Si}_{\text{As}}$ LVM also holds for excitation at 3.00 eV we have to conclude that scattering by the $^{29}\text{Si}_{\text{Ga}}$ LVM, which is dispersionless in the energy range 1.9–2.4 eV and not resolved for photon energies in the range 2.5–2.7 eV, has a sharp and strong resonance for photon energies close to the E_1 gap energy. However, the reasons for the differences in the resonance behavior of scattering by Si_{As} and Si_{Ga} LVM's are not yet clear. The question of whether these differences are related to the different electrical activity of Si_{As} (acceptor) and Si_{Ga} (donor) or to the different lattice sites is also open. On the other hand, the present results make clear why in all the previous Raman studies of Si LVM's in GaAs,^{3–5} where the spectra were excited with photon energies in the range 2.4–2.5 eV, the Si_{As} LVM was found as the dominant LVM line.

There are two other examples of resonant Raman scattering by LVM in the literature to compare with our present results. For the LVM of B in crystalline silicon Chandrasekar *et al.* found, within the experimental error, a constant intensity ratio between the LVM and the optical zone-center phonon line for all incident photon energies used (1.9–2.7 eV).¹⁶ This indicates the same dispersion of $|a|$ for the LVM and the intrinsic phonon in agreement with our present result for the $^{29}\text{Si}_{\text{As}}$ LVM

in GaAs:Si. For P in Ge, however, Contreras *et al.* report a much lower $(E_1, E_1 + \Delta_1)$ gap resonance for scattering by the P LVM than for scattering by the optical zone-center phonon.²⁴ The authors attribute this behavior to \mathbf{k} nonconservation in the Raman scattering mechanism of the LVM. These measurements were carried out on samples implanted with very high doses of P ($6 \times 10^{16} \text{ cm}^{-2}$) followed by pulsed laser annealing. Presumably these samples contain a higher concentration of residual lattice damage than the present ones, which might explain the difference to our results.

To derive the present resonance Raman data, we used the dielectric function measured on undoped GaAs (Ref. 12) also for the heavily Si-doped samples, as stated above. This assumption certainly introduces some uncertainty, because it is known that heavy doping also changes the dispersion of ϵ .²³ Heavy doping effects tend to smooth the dispersion of the dielectric function. If we assume similar effects for our present samples, this would lead to a further lowering of the experimentally found $(E_1, E_1 + \Delta_1)$ gap resonance in the LO-phonon scattering for the implanted material. But the comparison between the LVM and LO-phonon scattering in this material remains unaffected by this question.

B. Heavily doped MBE layers

In the previous section Raman spectra excited at 3.00 eV, which is at 77 K in direct resonance with the E_1 gap energy of GaAs,²⁰ were found to show scattering by both the Si_{As} and the Si_{Ga} LVM with the sensitivity enhanced by the E_1 gap resonance. Using this excitation, we observe Raman scattering by Si_{Ga} LVM also in heavily doped GaAs MBE layers which have a much lower Si content than the implanted and annealed samples. Figures 9(b) and 9(c) display Raman spectra of such layers for two different carrier concentrations (see Table I). Figure 9(a) shows for reference the spectrum of undoped GaAs. The spectra were recorded in the $x(y,z)\bar{x}$ scattering configuration, which suppresses the Γ_1 component of the second-order phonon spectrum.¹³ Figure 10 depicts the difference curves obtained by subtracting the spectrum of undoped GaAs from the spectra of the heavily doped GaAs layers. For both samples only scattering by the $^{28}\text{Si}_{\text{Ga}}$ LVM is observed at 384 cm^{-1} (Ref. 4). This is consistent with the good electrical activation of the Si dopant (see Table I) indicating only a small concentration of compensating defect centers such as, e.g., Si_{As} .¹⁰ From the signal-to-noise ratio in the spectrum of the sample with a free carrier concentration of $2.3 \times 10^{18} \text{ cm}^{-3}$ [Fig. 10(a)] we can infer a detection limit for Raman scattering by the Si LVM in GaAs of $\sim 10^{18} \text{ cm}^{-3}$ for measurements at 77 K.

It is interesting to note that we observe Raman scattering by the Si_{Ga} LVM in these MBE layers only for excitation at 3.00 eV and not for excitation below the E_1 gap resonance at, e.g., 2.71 eV. This indicates a rather narrow E_1 gap resonance for Raman scattering by the Si_{Ga} LVM also in this material, which gives support to the above results for Si-implanted and annealed GaAs.

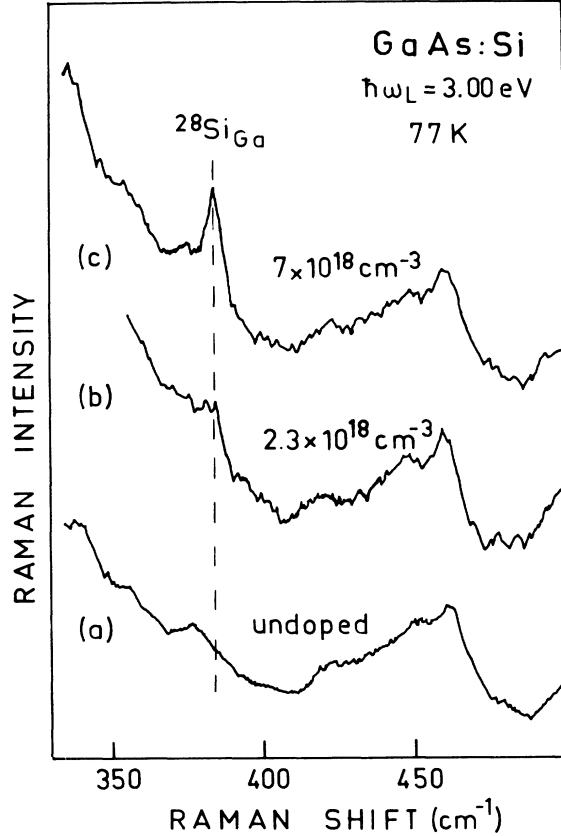


FIG. 9. Low-temperature (77 K) Raman spectra of Si-doped GaAs grown by MBE [(b) and (c)] and of undoped GaAs (a). The carrier concentrations given in the figure were deduced from Hall-effect measurements. The spectra were excited at 3.00 eV and recorded with a spectral resolution of 5 cm^{-1} . The scattering configuration was $x(y,z)\bar{x}$. $^{28}\text{Si}_{\text{Ga}}$ denotes Raman scattering by the $^{28}\text{Si}_{\text{Ga}}$ LVM.

On the other hand, the crystalline quality of Si-doped GaAs MBE layers is certainly better than that of high-dose ion-implanted and rapidly thermal annealed GaAs. Therefore the observation of Raman scattering by Si LVM's in MBE material forms a good basis for further Raman investigations of Si local vibrational modes in GaAs.

IV. CONCLUSIONS

We have used resonant Raman scattering to study Si local vibrational modes in ion-implanted and annealed as

TABLE I. Carrier concentrations measured by Hall effect (n_{Hall}) and by Raman scattering (n_{Raman}) as well as the total Si concentration measured by SIMS ($[\text{Si}]_{\text{SIMS}}$) for the MBE-grown GaAs samples used in this study.

MBE Sample no.	n_{Hall} (10^{18} cm^{-3})	n_{Raman} (10^{18} cm^{-3})	$[\text{Si}]_{\text{SIMS}}$ (10^{18} cm^{-3})
1	2.3 ± 0.4	3.8 ± 0.3	4.7 ± 1
2	7 ± 1.4	8.6 ± 0.3	12.0 ± 2

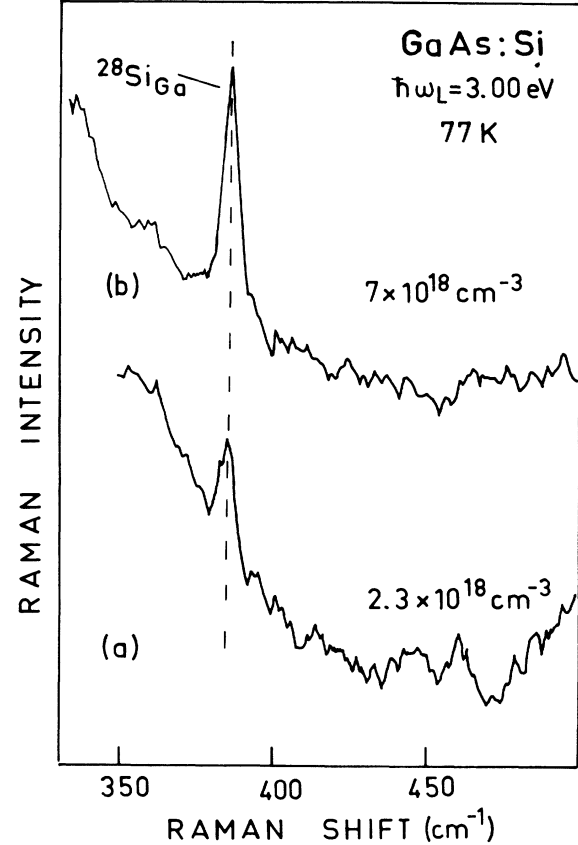


FIG. 10. Same spectra as in Figs. 9(b) and 9(c), but with the intrinsic second-order phonon spectrum subtracted.

well as MBE-grown GaAs. In ion-implanted material the same E_1 gap resonances were found for dipole-allowed LO-phonon scattering and for scattering by the Si_{As} LVM. Compared to undoped GaAs both resonances are considerably broadened. Scattering by the Si_{Ga} LVM, in contrast, shows a much narrower E_1 gap resonance. The reason for this difference in the resonance behavior is not yet known and further work is necessary to clarify that point. Using excitation resonant with the E_1 gap energy yields also Raman scattering of the Si_{Ga} LVM in Si-doped MBE-grown GaAs layers with a detection limit of $\sim 10^{18} \text{ cm}^{-3}$.

ACKNOWLEDGMENTS

We would like to thank J. Schaub and Ch. Hoffmann for implanting and annealing the samples and G. Bihlmann for help with the MBE growth. Thanks are also due to T. Fuchs for technical assistance with the SIMS measurements and to P. Koidl for many helpful discussions. We are further grateful to R. Murray and R. C. Newman for providing the LVM absorption data.

- ¹R. C. Newman, in *Festkörperprobleme XXV, Advances in Solid State Physics*, edited by P. Grosse (Vieweg, Braunschweig, 1985), p. 605.
- ²R. C. Newman, in *E-MRS Symposium Proceedings Vol. XIII*, edited by P. A. Glasow, Y. I. Nissim, J. P. Noblanc, and J. Speight (Les Editions de Physique, Le Ulis, France, 1986), p. 99.
- ³T. Nakamura and T. Katoda, *J. Appl. Phys.* **57**, 1084 (1985).
- ⁴M. Holtz, R. Zallen, A. E. Geissberger, and R. A. Sadler, *J. Appl. Phys.* **59**, 1946 (1986).
- ⁵T. Kamijoh, A. Hashimoto, H. Takano, and M. Sakuta, *J. Appl. Phys.* **59**, 2382 (1986).
- ⁶R. Ashokan, K. P. Jain, H. S. Mavi, and M. Balkanski, *J. Appl. Phys.* **60**, 1985 (1986).
- ⁷J. Wagner, M. Ramsteiner, and R. C. Newman, *Solid State Commun.* **64**, 459 (1987).
- ⁸W. M. Theis and W. G. Spitzer, *J. Appl. Phys.* **56**, 890 (1984).
- ⁹J. Woodhead, R. C. Newman, A. K. Tipping, J. B. Clegg, J. A. Roberts, and I. Gale, *J. Phys. D* **18**, 1575 (1985).
- ¹⁰J. Maguire, R. Murray, R. C. Newman, R. B. Beall, and J. J. Harris, *Appl. Phys. Lett.* **50**, 516 (1987).
- ¹¹G. Abstreiter, M. Cardona, and A. Pinczuk, in *Light Scattering in Solids IV*, edited by M. Cardona and G. Güntherodt (Springer, New York, 1984), p. 60.
- ¹²D. E. Aspnes and A. A. Studna, *Phys. Rev. B* **27**, 985 (1983).
- ¹³R. Trommer and M. Cardona, *Phys. Rev. B* **17**, 1865 (1978).
- ¹⁴T. Nakamura and T. Katoda, *J. Appl. Phys.* **53**, 5870 (1982).
- ¹⁵J. Wagner, M. Ramsteiner, and W. Haydl, *J. Appl. Phys.* **61**, 3050 (1987).
- ¹⁶M. Chandrasekar, H. R. Chandrasekar, M. Grimsditch, and M. Cardona, *Phys. Rev. B* **22**, 4825 (1980).
- ¹⁷See, e.g., M. Cardona, in *Light Scattering in Solids II*, edited by M. Cardona and G. Güntherodt (Springer, New York, 1982), p. 19.
- ¹⁸R. Murray and R. C. Newman (unpublished LVM absorption data).
- ¹⁹M. H. Grimsditch, D. Olego, and M. Cardona, *Phys. Rev. B* **20**, 1758 (1979).
- ²⁰S. O. Sari and S. E. Snatterly, *Surf. Sci.* **37**, 328 (1973).
- ²¹A. Compaan and H. J. Trodahl, *Phys. Rev. B* **29**, 793 (1984).
- ²²J. Menéndez and M. Cardona, *Phys. Rev. B* **31**, 3696 (1985).
- ²³A. K. Sood, G. Contreras, and M. Cardona, *Phys. Rev. B* **31**, 3760 (1985).
- ²⁴G. Contreras, A. Compaan, and A. Axmann, *J. Phys. (Paris) Colloq.* **44**, C5-193 (1983).